Article

Determination of Key Hydrocarbon Autoxidation Products By Fluorescence

Ron Shah, and Derek A. Pratt

J. Org. Chem., **Just Accepted Manuscript** • DOI: 10.1021/acs.joc.6b01032 • Publication Date (Web): 06 Jul 2016

Determination of Key Hydrocarbon Autoxidation Products By Fluorescence

Ron Shah & Derek A. Pratt*

Department of Chemistry and Biomolecular Sciences

University of Ottawa, Ottawa, Canada K1N 6N5

dpratt@uottawa.ca

Abstract: Hydroperoxides and carboxylic acids are key primary products that arise in the autoxidation of hydrocarbons. We have developed a simple approach to rapidly and simultaneously determine both types of products using hydroperoxide- and acid-sensitive moieties conjugated to non-polar coumarin- and BODIPY-based fluorophores. The coumarin- and BODIPY-conjugated amine probes described here undergo 38- and 8-fold enhancement, respectively, upon protonation in a solvent system compatible with heavy hydrocarbons. The latter can be used directly with our previously described hydroperoxide-sensitive coumarin-conjugated phosphine probe to enable rapid quantification of both carboxylic acids and hydroperoxides in hydrocarbon samples. The utility of the approach is illustrated by the ready determination of different relative rates of hydroperoxide and acid formation with changes in hydrocarbon structure (e.g. *n*-hexadecane *vs.* 1-hexadecene *vs.* a lubricant basestock). The method offers significant versatility and automation compared to common, but laborious titration approaches and greatly improves screening efficiency and accuracy for the identification of novel radical-trapping antioxidants for high temperature applications. This application was demonstrated by the automated analysis of hydroperoxides and carboxylic acids (by microplate reader) in samples from 24 inhibited autoxidations of a lubricating oil, which were carried out on a parallel synthesizer at 160°C in triplicate in a single day.

Introduction

Autoxidation is the spontaneous radical-mediated process that converts hydrocarbons into their corresponding hydroperoxides (Scheme 1). It is primarily responsible for the degradation of all hydrocarbon-based products such as plastics, rubbers and lubricants.[1]

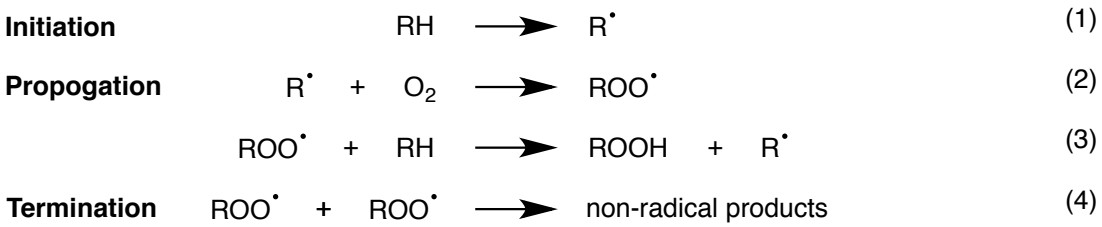

Scheme 1: Hydrocarbon autoxidation.

The sequence of reactions in Scheme 1 (in particular Eq. 2-3) constitutes a generalized, but also greatly simplified, mechanism of hydrocarbon autoxidation. In fact, the primary products of autoxidation are not simply monohydroperoxides and the secondary products involve cleavage of carbon-carbon bonds. In fact, as first demonstrated by Korcek and co-workers for the autoxidation of *n*-hexadecane, ketohydroperoxides (of which the γ-isomer is predominant) are formed competitively from very early on, and carboxylic acids and methyl ketones shortly thereafter.[2] The formation of each of these products can be rationalized by the mechanism in Scheme 2.[3]

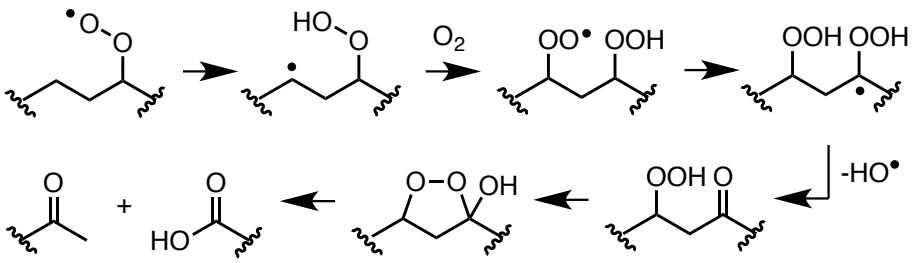

Scheme 2: Proposed mechanism of acid formation in *n*-alkane autoxidation.

The accumulation of these autoxidation products (or subsequent decomposition products thereof) can alter the properties of hydrocarbon-based products and/or materials that come into contact with them. For instance, autoxidation of engine lubricants increases their viscosity and the production of acids leads to corrosion of metallic engine parts. As such, antioxidants are key additives to essentially all hydrocarbon-based materials. Radical-trapping antioxidants (RTAs, A-H in Eq. 5), such as phenols and aromatic amines, intervene directly in the radical chain-reaction depicted in Scheme 1 by reducing the chain-carrying peroxyl radicals by H-atom transfer, thereby precluding chain-propagation.[4,5]

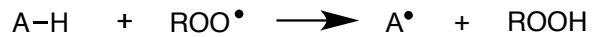

(5)

In an attempt to speed up the identification and assessment of new chemical entities as RTAs, we recently reported a strategy to monitor the production of hydroperoxides using fluorogenic phosphine **1**.[6] This probe enables rapid quantification of hydroperoxides by measuring the pseudo-first order rate of fluorescence increase in a microplate assay instead of more conventional methods, such as iodometric titration (i.e. ASTM method D3703-13) or lengthy HPLC or GC analyses.[7] This method has proven highly useful in quantifying hydroperoxides,[8-11] but ignores the acids that are produced. In addition to their role in advancing corrosion, carboxylic acids can have a profound impact on both the kinetics and mechanisms of the RTAs added to protect the substrate from autoxidation (e.g. diarylamines[9] and hindered amine light stabilizers[10]). Thus, we have extended our work on **1** (Scheme 3) to the development of an analogous strategy to monitor the production of carboxylic acids in hydrocarbon autoxidations, which are conventionally determined by acid-base titration (i.e. ASTM method D664-11a).[12]

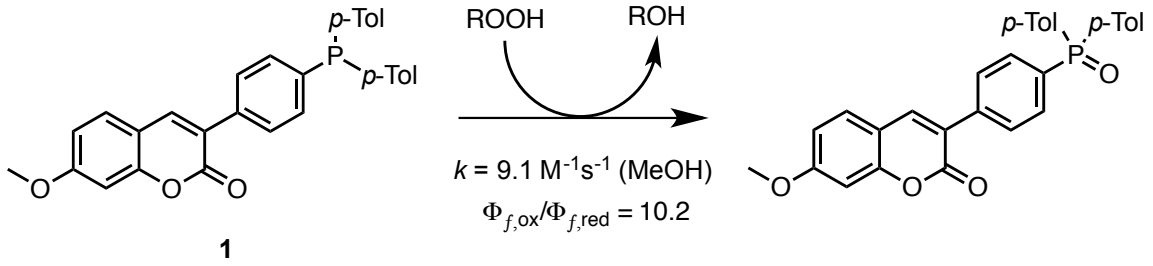

Scheme 3: The reaction of fluorogenic coumarin-triarylphosphine **1** with hydroperoxides.

Although acid-sensitive fluorescent probes have been developed for the real-time monitoring of intracellular pH by flow cytometry or fluorescence microscopy, they are unsuitable for monitoring acid production in the current context for solubility reasons.[13-21] Moreover, the probes reported to date are relatively complex, and we envisioned simply using the same trivially accessed 7-methoxycoumarin core as in hydroperoxide probe **1**. We surmised that a similar probe wherein the triarylphosphine moiety was replaced with a basic trialkylamine unit would undergo fluorescence enhancement with increasing acidity of the medium, similarly to the response of **1** to increasing hydroperoxide concentration. The electron-rich trialkylamine is expected to quench the fluorescence of the coumarin by photoinduced electron transfer (P*e*T); protonation would preclude P*e*T.[22]

Results and Discussion

Coumarin **2** was easily prepared (see Experimental Section), and as expected, its fluorescence was dramatically increased upon protonation (Figure 1B). Determination of the fluorescence of **2** as a function of pH yielded a sigmoidal profile whose midpoint indicates a ${}^{s}_{s}pK_a$ of 7.9±0.1 (Figure 1B). The experiments were carried out in 4:1 MeOH:*i*-PrOH (v:v) to ensure a balance between solubility of hydrocarbon samples (*vide*

infra), efficient quenching of coumarin fluorescence by PeT, and ionizability of **2**. It should be noted that this solvent mixture is characterized by an autoprotolysis constant of 15.3 and associated neutrality at ${}^{s}_{s}pH$ = 9.2.[23] Under these conditions, the ratio of fluorescence quantum yields of **2** and its conjugate acid (**2**-$\mathbf{H}^+$) was determined to be 38 (Figure 1C).

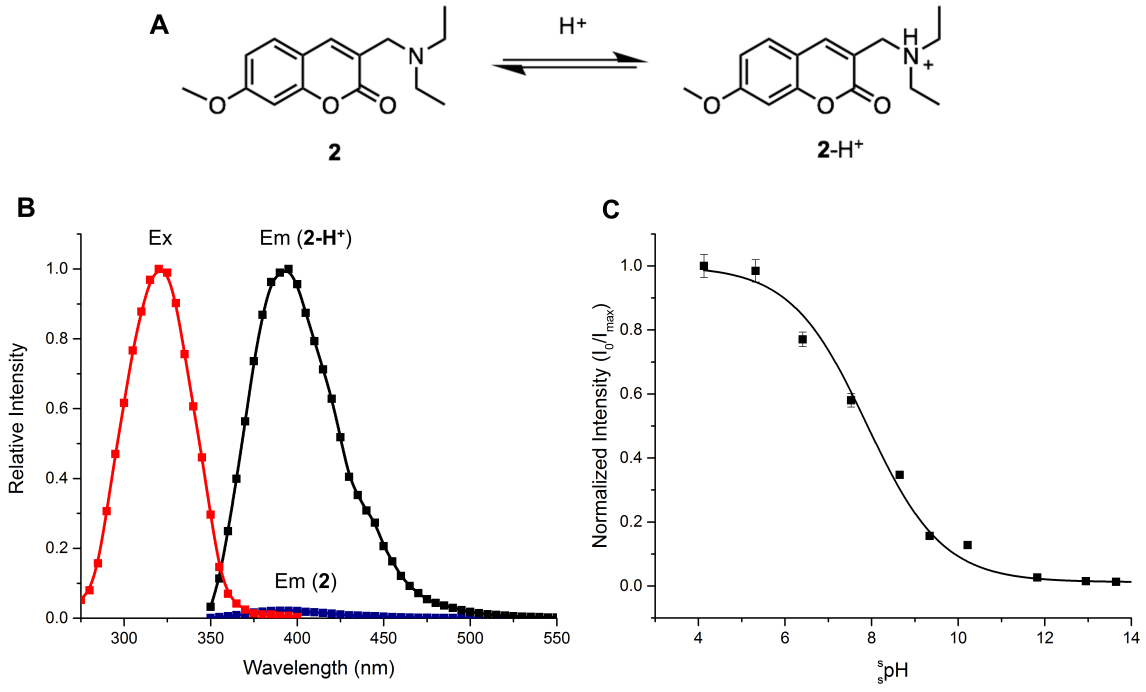

Figure 1. (**A**) The relevant equilibrium of the coumarin-trialkylamine **2** and its conjugate acid **2**-$\mathbf{H}^+$. (**B**) Excitation and emission spectra of **2** and **2**-H^+. (**C**) Fluorescence of **2** (λ_{ex} = 315 nm; λ_{em} = 395 nm) as a function of pH in 4:1 MeOH:*i*-PrOH.

The foregoing suggested that carboxylic acid formation could be monitored in autoxidation samples simply by determination of their fluorescence following addition of **2** and dissolution in the 4:1 MeOH:*i*-PrOH solvent system.[24] Figure 2A reveals the linear relationship between the fluorescence of **2** and added palmitic acid, a representative

lipophilic carboxylic acid. Based on this standard, carboxylic acid formation in the initial stages of an *n*-hexadecane autoxidation (carried out at 160°C in a stirred flow reactor)[2,6,25] were readily determined and yielded similar results to those obtained previously by (negative ion) electrospray mass spectrometric analysis (Figure 2B).[9] The previous results involved determination of each individual isomer of carboxylic acid formed in the *n*-hexadecane autoxidations from the mass spectra, and then summing them in order to determine the total acid concentration.[26,27] It should be noted that **2** does not react with hydroperoxides (see the Supporting Information for the results of the control experiments).

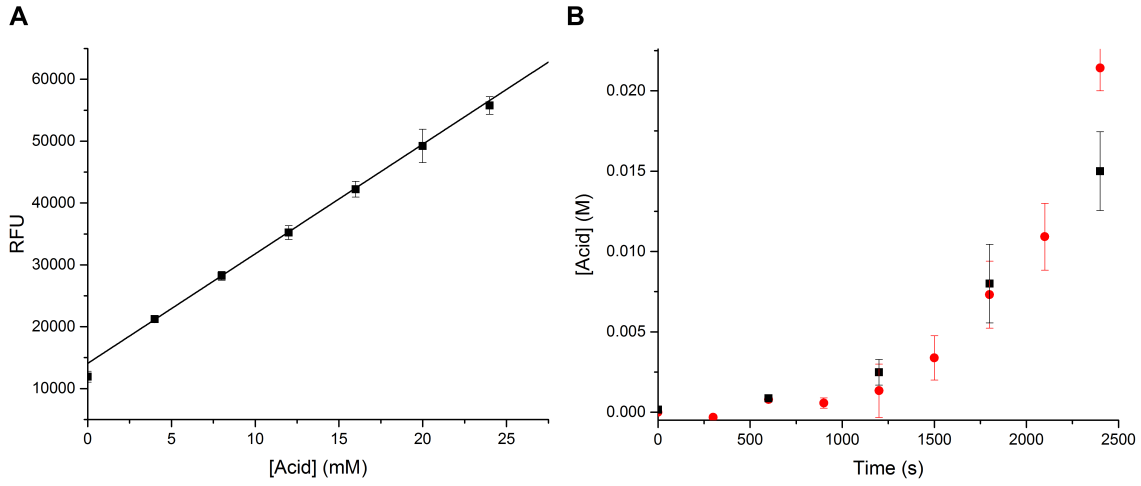

Figure 2. (**A**) Fluorescence of **2** (λ_{ex} = 315 nm; λ_{em} = 395 nm) determined as a function of palmitic acid concentration in 4:1 MeOH:*i*-PrOH. (**B**) Acid formation in the initial stages (<2% conversion) of an *n*-hexadecane autoxidation at 160˚C determined directly by ESI-MS (■) or indirectly by the fluorescence of **2** (●).

n-Hexadecane is a convenient model for heavy hydrocarbon autoxidation because it produces the simplest possible product distribution. In fact, industrial and/or

commercially relevant hydrocarbon-based products are usually mixtures of compounds and/or constitutional isomers. Since the current method does not require knowledge of the precise structure of each of the carboxylic acid products that are formed, acid production can easily be determined in these complex mixtures. An example is shown in Figure 3 where acid formation was determined in the initial stages of the autoxidation of a lubricant basestock (an American Petroleum Institute Group III base oil) at 160°C.[28] The hydroperoxides were determined in parallel (using **1**), and are shown on the same plot (Fig. 3B) alongside the corresponding data for an *n*-hexadecane autoxidation (Fig. 3A).

The data reveal that the base oil is more easily oxidized than *n*-hexadecane. However, less acid is produced relative to hydroperoxide at these early stages of the autoxidation. These results can be understood on the basis that the base oil contains branched hydrocarbons and that H-atom abstraction from tertiary positions of hydrocarbons by peroxyl radicals is faster than from secondary positions (i.e. $k = 7.0\times10^{-3}$ and 1.5×10^{-4} $M^{-1}s^{-1}$ for H-atom abstraction from the tertiary and secondary positions of 2-methylbutane, respectively, at 30°C)[29] and this is the rate-determining propagation step (Eq. 3) in the autoxidation. Moreover, the initially formed tertiary peroxyl radicals cannot undergo the sequence of reactions to form carboxylic acids as in Scheme 2; only the fraction of secondary peroxyl radicals that are formed – and that undergo intramolecular H-atom abstraction from a secondary site in lieu of intermolecular propagation by abstraction at a tertiary site – can contribute via this pathway. Of course, it must be acknowledged that acids may arise from other mechanisms.

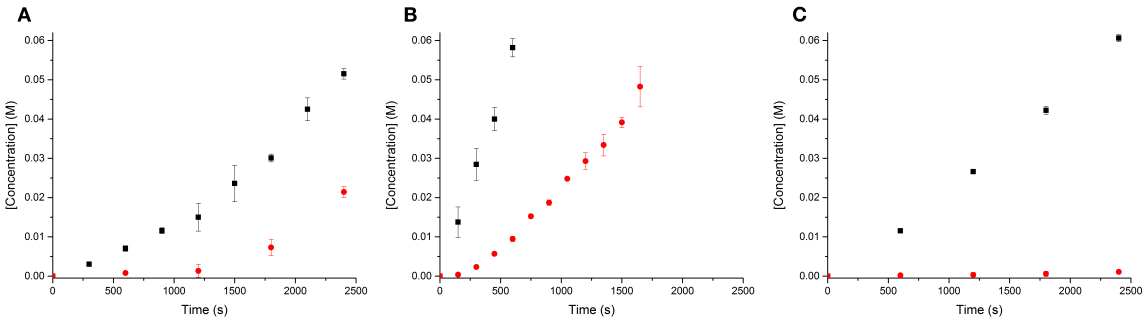

Figure 3. Formation of hydroperoxides (■) and acids (●) in the initial stages (<2% conversion) of the autoxidation of either *n*-hexadecane (**A**) or a API Group III base oil (**B**) at 160°C or 1-hexadecene (**C**) at 120°C. Autoxidations of *n*-hexadecane and base oil were initiated with tetralin hydroperoxide at 10 and 5 mM, respectively, while the 1-hexadecene autoxidations were initiated with 10 mM dicumyl peroxide.

The results of corresponding autoxidations of 1-hexadecene, a model α-olefin, are shown in Fig. 3C. These autoxidations were carried out at 120°C since 1-hexadecene is an unsaturated hydrocarbon that oxidizes much more rapidly than saturated ones, such as *n*-hexadecane (i.e. k_p = 1 $M^{-1}s^{-1}$ for 1-octene *vs.* k_p = 0.0015 $M^{-1}s^{-1}$ for *n*-octane at 30°C).[30,31] Very little acid is produced relative to hydroperoxide in the early stages of these autoxidations – presumably since intermolecular propagation is much faster than intramolecular H-atom abstraction. The production of acid via the mechanism in Scheme 2 requires the intramolecular H-atom abstraction from an unactivated position to compete with the intermolecular H-atom abstraction from an allylic position – which is unlikely. Indeed, ESI-MS measurements of samples from the 1-hexadecene autoxidation (Fig. 4B) reveal a very different profile of acids that are formed compared to that observed from samples of the *n*-hexadecane autoxidation (cf. Fig. 4A), implying that the mechanism of

acid formation in 1-hexadecene autoxidations is very different than in autoxidations of linear saturated hydrocarbons. The two most predominant peaks in the mass spectra are consistent with the molecular formulas of hexadeca-2-enoic acid and *n*-pentadecanoic acid, which may derive from the expected allylic hydroperoxide arising in the autoxidation of 1-hexadecene as is shown in Scheme 4.[32]

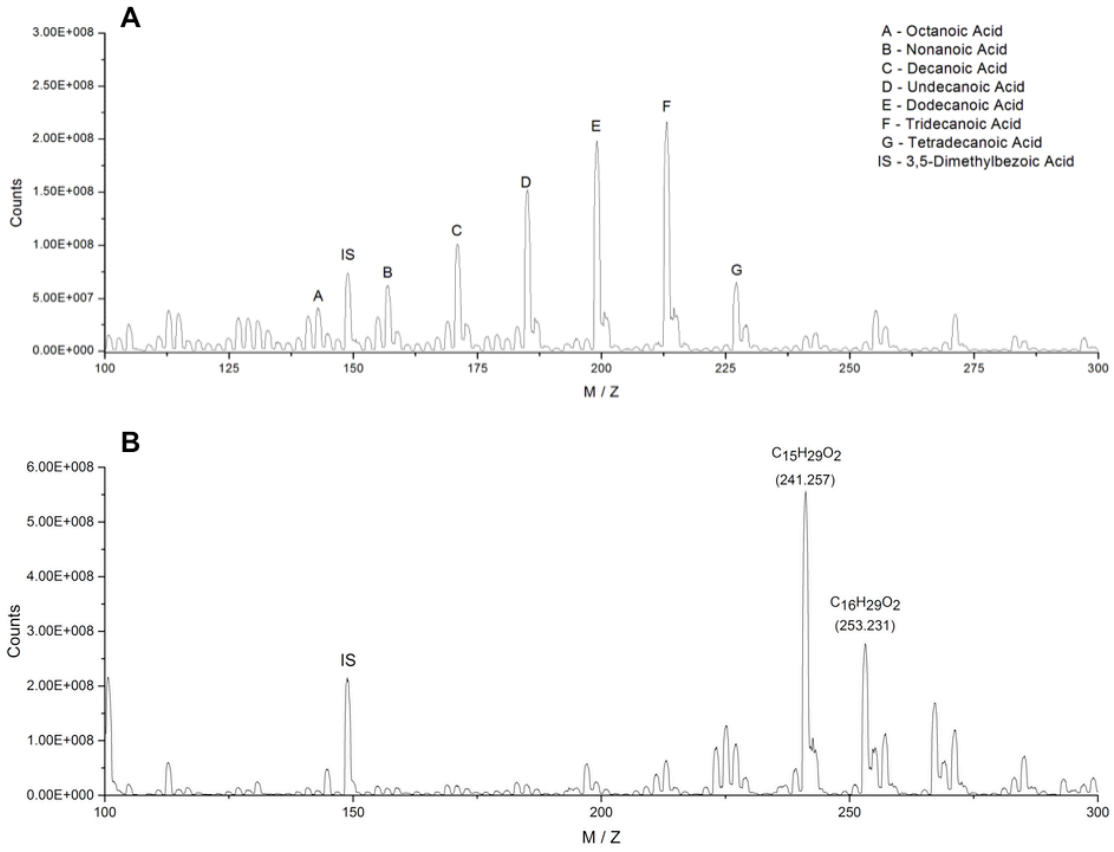

Figure 4. Representative negative ion electrospray mass spectra from the initial stages of autoxidations of either *n*-hexadecane (**A**) or 1-hexadecene (**B**) at 160°C and 120 °C, respectively. Samples (50 μL) were withdrawn 2400 or 4800 s into the autoxidation, diluted with 4.95 mL of a 20% i-PrOH/80% MeOH solution containing 3,5-dimethylbenzoic acid (10.5 μM) as an internal standard.

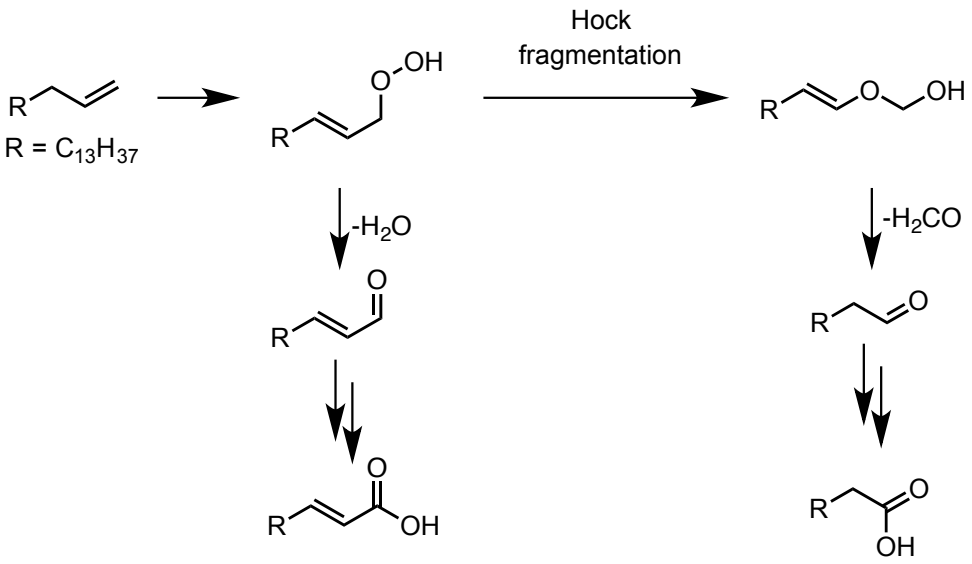

Scheme 4: Possible mechanisms for the formation hexadeca-2-enoic acid and *n*-pentadecanoic acid in the autoxidation of 1-hexadecene.

Our motivation for the development of rapid means to quantify hydroperoxides[6] – and now acids – in hydrocarbon autoxidations was the ability to assess the efficacy of RTAs. In Figure 5, we show the results of inhibited autoxidations of the same three model hydrocarbons (*n*-hexadecane, the API Group III base oil and 1-hexadecene) in the presence of diarylamines **3** and **4**. Compound **3** is an alkylated diphenylamine representative of catalytic diarylamine antioxidants found in a variety of hydrocarbon-based products (e.g. lubricating oils and rubber) and compound **4** is representative of a recently developed class of heterocyclic diarylamines that have been shown to better inhibit hydrocarbon autoxidation compared to industry standards.[9,33-36]

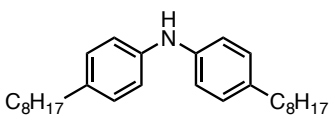

3

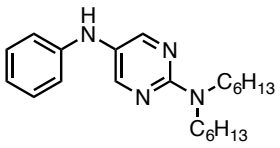

4

The increased reactivity of the heterocyclic diarylamine **4** relative to **3** is readily observed in Figures 5A and B, where **4** was able to suppress acid formation to a greater extent than **3** in each of *n*-hexadecane and the API Group III base oil, respectively. The same trend is observed in the inhibition of 1-hexadecene autoxidation (Figure 5C), but because acid formation lags considerably behind hydroperoxide formation in 1-hexadecene (*cf.* Figure 4), resolution of the difference requires running the autoxidation to much higher conversion.

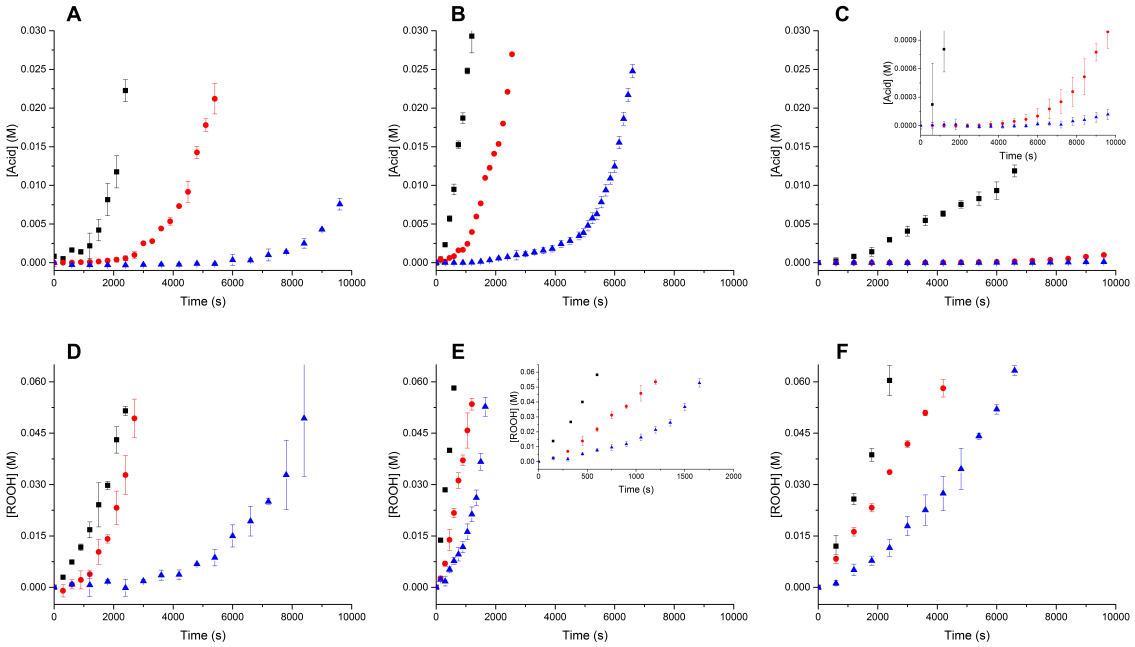

Figure 5. Formation of carboxylic acids (**A**-**C**) and hydroperoxides (**D**-**F**) in the autoxidation of either *n*-hexadecane (**A**,**D**) or a API Group III base oil (**B**,**E**) at 160˚C or 1-hexadecene (**C**,**F**) at 120˚C (■) and corresponding data for autoxidations inhibited by either **3** (●) or **4** (▲) at 40 μM in *n*-hexadecane and 1-hexadecene and 100 μM in base oil. Autoxidations of *n*-hexadecane and base oil were initiated with tetralin hydroperoxide at 10 and 5 mM, respectively, while the 1-hexadecene autoxidations were initiated with 10 mM dicumyl peroxide. Autoxidations were carried out in the presence of 2,4,6-tri-*tert*-

butylpyridine (1 mM) in order to prevent deactivation of **4** by acid formed during the autoxidation (see ref. 9).

The corresponding hydroperoxide analyses of the inhibited autoxidation samples using the fluorogenic phosphine **1** are shown in Figures 5D-F. Interestingly, the heterocyclic diarylamine **4** appears to be more effective than the diphenylamine standard **3** at inhibiting hydroperoxide formation in the *n*-hexadecane autoxidation relative to the base oil autoxidation, even though the profiles are similar when one considers acid formation only. Since the base oil autoxidizes so rapidly, it is more difficult for the antioxidants to compete with propagation (at this antioxidant loading). However, since acid formation is relatively slower (*cf.* Figure 4), the differences in the antioxidant efficacy are better resolved.

In the foregoing experiments, hydroperoxides and acids were determined in parallel. That is, duplicate samples were withdrawn from the hydrocarbon autoxidation, added to separate wells of a microplate and solutions of either **1** or **2** were added to one or the other and the fluorescence recorded. For operational expediency, and to limit the amount of material that must be used for analysis, it would be desirable to carry out both measurements on a single sample. However, since the fluorophores in **1** and **2** have practically identical properties, this is not possible. Hence, we prepared the BODIPY-substituted trialkylamine **5** (Figure 6) and examined its potential as an alternative to **2**.[13,37]

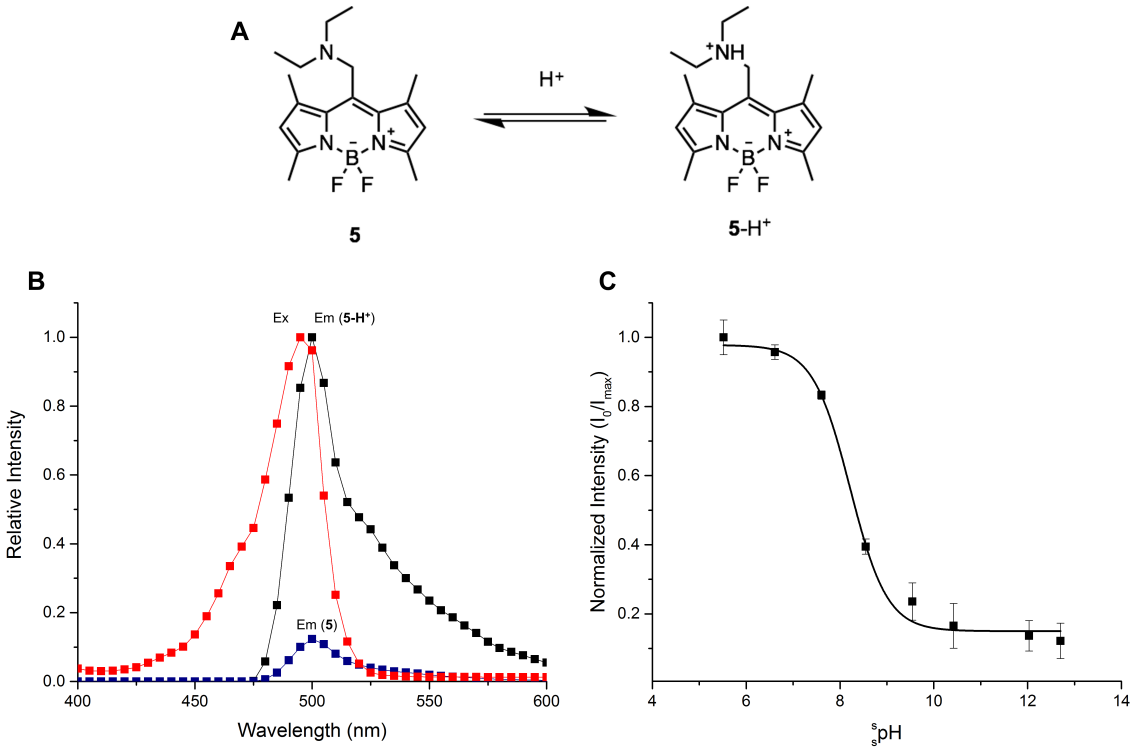

Figure 6. (**A**) The relevant equilibrium of the BODIPY-trialkylamine **5** and its conjugate acid **5-H**$^+$. (**B**) Excitation and emission spectra of **5** and **5-H**$^+$. (**C**) Fluorescence of **5** (λ_{ex} = 495; λ_{em} = 500) as a function of pH in 1:4 isopropanol/methanol.

Although the fluorescence enhancement observed upon protonation was less than for **2** (i.e., $\Phi_{\mathbf{5}\text{-H+}}/\Phi_{\mathbf{5}} = 8$ *vs.* $\Phi_{\mathbf{2}\text{-H+}}/\Phi_{\mathbf{2}} = 38$), it could be used interchangeably (i.e., ${}^{s}_{s}pK_a$ = 8.1±0.2 for **5** *vs.* 7.9±0.1 for **2** in in 4:1 MeOH:*i*-PrOH) and yielded essentially identical results for the foregoing experiments (see Supporting Information for the data).

To illustrate how this dual-approach is amenable to rapid screening of antioxidant efficacy, we carried out 24 inhibited autoxidations of base oil at 160˚C simultaneously in a commercial parallel reactor system that was adapted in-house to enable continuous oxygenation of all 24 reaction vessels. The reactions were supplemented with either of

twelve different aromatic amines (**6-17**) or twelve different phenols (**18-29**). The aromatic amines were assessed at lower loadings than the phenols (250 μM *vs.* 1 mM) since they are known to trap multiple radicals at elevated temperature due to a catalytic mechanism wherein the substrate can be used to regenerate the amine.[8,38] An aliquot from each reaction vessel was taken one-hour post initiation and acid and hydroperoxide concentrations were determined using probes **1** and **5** simultaneously using a microplate reader. The entire experiment was completed in triplicate in a single day.

The data in Figure 7 indicate that, consistent with our previous (significantly lower throughput) studies,[9] the heterocyclic diarylamines **6-10** all outperform the representative industrial standard dialkylated diphenylamine **11**. Similarly reactive to the heterocyclic diarylamines is phenoxazine (**14**), which was significantly better than its sulfur analog phenothiazine (**15**). Interestingly, liproxstatin-1 (**13**), one of the most potent inhibitors of cellular lipid peroxidation known,[39] is also particularly effective at inhibiting hydrocarbon autoxidations at high temperatures, while ferrostatin-1 (**12**), a similarly potent antioxidant in cell culture,[40] is noticeably less effective.

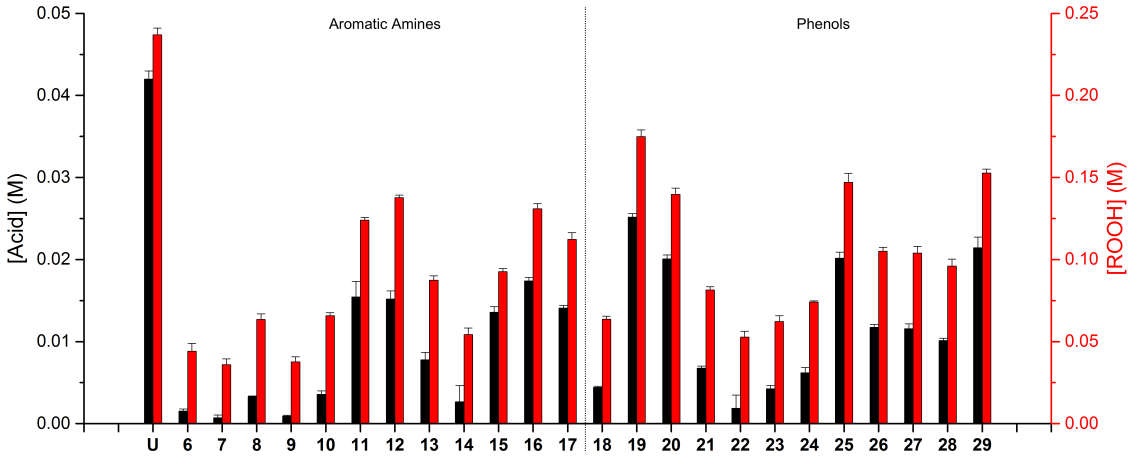

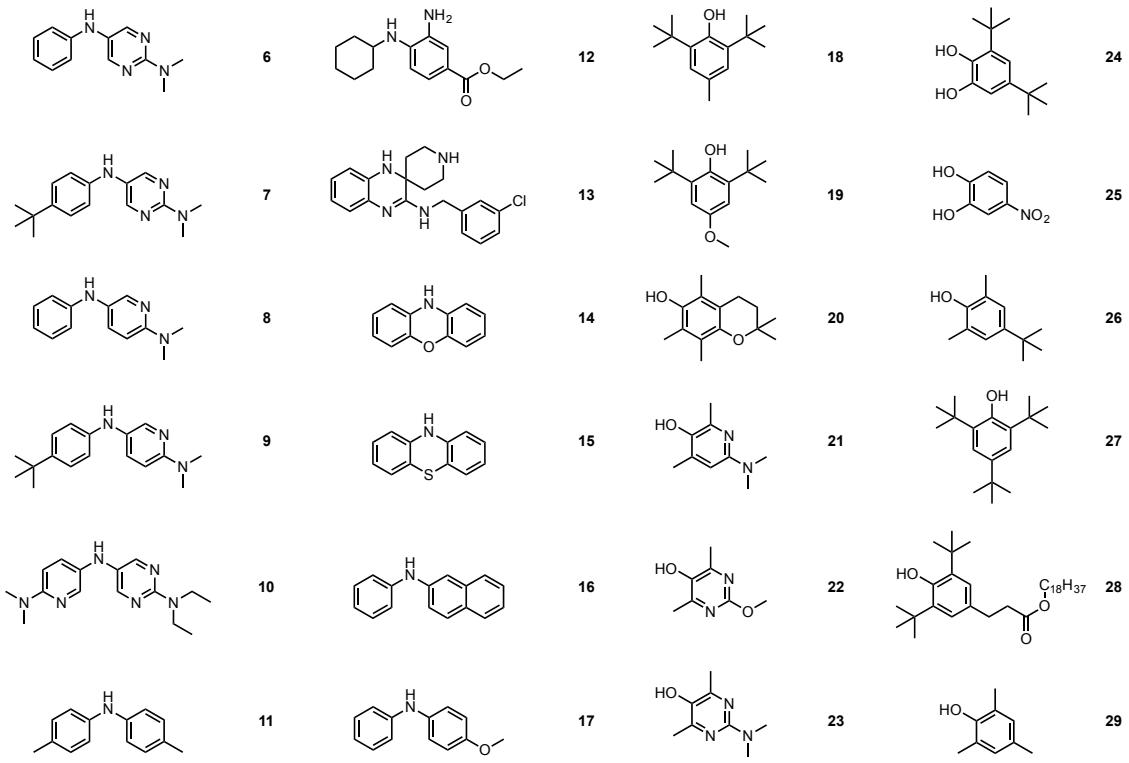

Figure 7. Formation of carboxylic acids (black) and hydroperoxides (red) upon autoxidation of a API Group III base oil for one hour at 160˚C (U = uninhibited) and corresponding data for autoxidations inhibited by either 250 μM of aromatic amines **6**-**17** or 1 mM of phenols **18**-**29**. Autoxidations were initiated with 5 mM tetralin hydroperoxide and carried out in the presence of 2,4,6-tri-*tert*-butylpyridine (1 mM).[41]

On the other hand, of the phenolic antioxidants we investigated, only pyrimidinols **22** and **23** suppressed autoxidation to a larger extent compared to the representative industrial standard BHT, **18**, which was similar to the di-*tert*-butylated catechol **24**. Despite the exciting reactivity of pyrimidinols as radical-trapping antioxidants at ambient temperatures,[42,43] they have yet to be studied at elevated temperatures. This result, and those obtained for phenoxazine and liproxstatin-1, underscore the value of this rapid

assessment of high temperature RTA activity for further, more detailed, investigations of promising compounds or classes of compound. Given that these analyses are generally carried out in both industry and academic laboratories by laborious iodometric and acid-base titrations, respectively, we anticipate that this will be a widely adopted screening tool for the identification of useful compounds and unanticipated conceptually novel chemistry.

Experimental Section

General

Reagents were purchased from commercial suppliers and used without further purification, unless otherwise indicated. Column chromatography was carried out using flash silica gel (40-63 μm, 230-400 mesh). ^{1}H and ^{13}C NMR were recorded on a spectrometer operating at 400 MHz and 100 MHz spectrometer, respectively, unless specified otherwise. High-resolution mass spectra were obtained on a magnetic sector electron impact mass spectrometer.

3-((Diethylamino)methyl)-7-methoxy-2H-chromen-2-one (2). To a solution of 3-(Bromomethyl)-7-methoxy-2H-chromen-2-one[45] (0.53 g, 2.0 mmol), KI (0.033 g, 0.2 mmol) and K_2CO_3 (0.4 g,3 mmol) in THF (20 mL) diethylamine (0.24 mL, 2.4 mmol) was added dropwise. The reaction was stirred overnight at room temperature until completion as determined by TLC. The mixture was added to a separatory funnel and extracted using Et_2O and water. The organic layer was dried over $MgSO_4$, filtered and the solvent was evaporated under vacuo. Column chromatography (25% Et_2O/Hexanes eluent) afforded pure product. Yield: 0.45 g, 86%. Brown Oil. ^{1}H NMR (400 MHz;

aceton-d6): δ 7.90 (s, 1H), 7.59 (d, *J* = 8.5 Hz, 1H), 6.93-6.88 (m, 2H), 3.91 (s, 3H), 3.41 (d, *J* = 1.3 Hz, 2H), 2.58 (q, *J* = 7.1 Hz, 4H), 1.05 (t, *J* = 7.1 Hz, 6H). ^{13}C NMR (100 MHz; aceton-d6): δ 163.0, 161.6, 155.6, 139.8, 129.6, 124.9, 114.0, 112.9, 101.0, 56.2, 52.6, 48.2, 12.6. HRMS: m/z Calc: $C_{15}H_{19}NO_3$: 261.1365 Found: 261.1369.

7-Methoxy-3-methyl-2H-chromen-2-one. The precursor to 3-(bromomethyl)-7-methoxy-2H-chromen-2-one[45] used in the synthesis of **2** was prepared using a previously reported procedure with slight modifications.[44] Ethyl 2-(triphenylphosphoranylidene)propanoate (0.9 g, 6.0 mmol) and 2-hydroxy-4-methoxybenzaldehyde (2.1 g, 6.0 mmol) were stirred in a sealed tube and heated to 200˚C overnight. The reaction was cooled and the crude product was recrystallized from chloroform and hexanes. Yield: 1.05 g, 92%. Brown needles. ^{1}H-NMR (400 MHz; aceton-d6): δ 7.69 (s, 1H), 7.49 (d, *J* = 8.5 Hz, 1H), 6.91-6.86 (m, 2H), 3.90 (s, 3H), 2.09 (s, 3H). NMR spectra were consistent with previously reported data.[44]

10-((Diethylamino)methyl)-5,5-difluoro-1,3,7,9-tetramethyl-5H-dipyrrolo[1,2-c:2',1'-f][1,3,2]diazaborinin-4-ium-5-uide (5). To a solution of 10-(chloromethyl)-5,5-difluoro-1,3,7,9-tetramethyl-5*H*-4λ^4,5λ^4-dipyrrolo[1,2-*c*:2',1'-*f*][1,3,2]diazaborinine[13] (0.1 g, 0.3 mmol), KI (0.005 g, 0.03 mmol) and K_2CO_3 (0.062 g, 0.45 mmol) in THF (3 mL) diethylamine (0.037 mL, 0.36 mmol) was added dropwise. The reaction was stirred overnight at room temperature until completion as determined by TLC. The mixture was added to a seperatory funnel and extracted using Et_2O and water. The organic layer was dried over $MgSO_4$, filtered and the solvent was evaporated under vaccuo. Column chromatography (25% Et_2O/Hexanes eluent) afforded pure product. Yield: 0.042 g, 42%. Orange solid. ^{1}H NMR (400 MHz; aceton-d6): δ 6.45 (s, 1H), 6.17 (s, 1H), 3.83 (s, 2H),

2.66 (s, 3H), 2.58 (q, J = 7.1 Hz, 4H), 2.48 (s, 3H), 2.45 (s, 6H), 1.04 (t, J = 7.1 Hz, 6H). ^{13}C NMR (76 MHz; aceton-d6): δ 158.5, 154.0, 143.8, 142.4, 142.1, 132.7, 122.0, 120.8, 51.8, 48.7, 17.5, 17.3, 16.7, 14.4, 12.6. Calc: $C_{18}H_{26}BF_2N_3$: 333.2188 Found: 333.2189.

General Procedure for Hydrocarbon Autoxidations

n-Hexadecane, 1-hexadecene or the base oil (100 mL) were thoroughly degassed with argon and then heated to 160°C in a stirred flow reactor. Once the temperature stabilized, inhibitor **3** or **4**, base (2,4,6-tri-*tert*-butylpyridine, 1 mM final concentration) and an appropriate amount of initiator (see text) were added to the solution and the flow of argon was replaced with O_2. Aliquots (0.5 mL) were withdrawn every 5 minutes, and allowed to cool to room temperature for analysis.

General Procedure for Determining Hydroperoxide Concentration

Four replicates (30 μL) of each sample were loaded into separate wells of a 96-well microplate and the automated reagent dispenser of the microplate reader was used to dilute each sample with *tert*-amyl alcohol (200 μL) and a solution of a fluorgenic phosphine dye **1** (20 μL of a 250 μM stock solution in acetonitrile) immediately before reading. The plate was stirred for 8 seconds, and allowed to rest for 2 seconds, and the fluorescence of each well was measured every second for 60 seconds (excitation wavelength = 340 nm; emission wavelength = 425 nm). The concentration of hydroperoxide was determined from the rate of phosphine oxidation using the rate constant for the reaction of the dye with secondary hydroperoxides in *tert*-amyl alcohol (k = 1.2 $M^{-1}s^{-1}$) assuming pseudo-first-order kinetics.

General Procedure for Determining Acid Concentration

Four replicates (1.2 μL) of each sample were loaded into separate wells of a 96-well microplate and the automated reagent dispenser of the microplate reader was used to dilute each sample with 20% isopropyl alcohol in methanol (280 μL), and the plate was stirred for 15 s. Afterward, a solution of fluorogenic amine **2** (20 μL of a 630 μM stock in methanol) was added. The plate was stirred for 8 s, and the fluorescence of each well was measured every second for 10 s (excitation wavelength = 315 nm; emission wavelength = 395 nm) and the acid concentration was determined from the average fluorescence reading (RFU = 1771 [Acid] + 14065).

General Procedure for Simultaneous Determination of Hydroperoxide and Acid Concentration

Four replicates (5 μL) of each sample were loaded into separate wells of a 96-well microplate and the automated reagent dispenser of the microplate reader was used to dilute each sample with 20% isopropyl alcohol in methanol (280 μL), and the plate was stirred for 15 s. Afterward, a solution containing fluorogenic phosphine dye **1** and fluorogenic amine **5** (20 μL of a solution containing 250 μM of probe **1** and 630 μM of probe **5** in acetonitrile) were added. The plate was stirred for 8 s, and the fluorescence of each well was measured every five seconds for 60 s (excitation wavelength = 340 nm; emission wavelength = 425 nm for probe **1** and excitation wavelength = 495 nm; emission wavelength = 500 nm for probe **5**). The acid concentration was determined from the average fluorescence reading over 10 s (RFU = 352 [Acid] + 34925). The concentration of hydroperoxide was determined from the rate of phosphine oxidation

using the rate constant for the reaction of the dye with secondary hydroperoxides in 20% isopropyl alcohol in methanol (k = 5.1 $M^{-1}s^{-1}$) assuming pseudo-first-order kinetics.

Screening of High Temperature Antioxidant Activity

Base oil (3 mL) was added to test tubes in a 24-place parallel synthesizer, thoroughly degassed with argon and then heated to 160°C. Once the temperature stabilized, an appropriate amount of inhibitor **6-29** (see text), base (2,4,6-tri-*tert*-butylpyridine, 1 mM final concentration) and 5 mM tetralin hydroperoxide were added to the test tubes and the flow of argon was replaced with O_2. An aliquot (0.1 mL) was withdrawn 1-hour post initiation, and allowed to cool to room temperature for analysis.

Supporting Information. Standardization data, results of autoxidations analysed using **5** and relevant NMR spectra. This material is available free of charge on the ACS Publications website.

Acknowledgement. We acknowledge the support of the Natural Sciences and Engineering Research Council (NSERC) of Canada and the Canada Foundation for Innovation. DAP also acknowledges support from the University of Ottawa and the Canada Research Chairs program, respectively, while RS acknowledges the support of NSERC in the form of a Canada Graduate Scholarship.

References

(1) Bateman, L. *Q. Rev. Chem. Soc.* **1954**, *8*, 147.
(2) Jensen, R. K.; Korcek, S.; Mahoney, L. R.; Zinbo, M. *J. Am. Chem. Soc.* **1979**, *101*, 7574.

(3) Jalan, A.; Alecu, I. M.; Meana-Pañeda, R.; Aguilera-Iparraguirre, J.; Yang, K. R.; Merchant, S. S.; Truhlar, D. G.; Green, W. H. *J. Am. Chem. Soc.* **2013**, *135*, 11100.
(4) Ingold, K. U. *Chem. Rev.* **1961**, *61*, 563.
(5) Ingold, K. U.; Pratt, D. A. *Chem. Rev.* **2014**, *114*, 9022.
(6) Hanthorn, J. J.; Haidasz, E.; Gebhardt, P.; Pratt, D. A. *Chem. Commun.* **2012**, *48*, 10141.
(7) *Standard Test Method for Hydroperoxide Number of Aviation Turbine Fuels, Gasoline and Diesel Fuels*; ASTM International: West Conshohocken, PA.
(8) Haidasz, E. A.; Shah, R.; Pratt, D. A. *J. Am. Chem. Soc.* **2014**, *136*, 16643–16650.
(9) Shah, R.; Haidasz, E. A.; Valgimigli, L.; Pratt, D. A. *J. Am. Chem. Soc.* **2015**, *137*, 2440.
(10) Haidasz, E. A.; Meng, D.; Amorati, R.; Baschieri, A.; Ingold, K. U.; Valgimigli, L.; Pratt, D. A. *J. Am. Chem. Soc.* **2016**, *138*, 5290.
(11) Li, B.; Zheng, F.; Chauvin, J.-P. R.; Pratt, D. A. *Chem. Sci.* **2015**, *6*, 6165.
(12) *Test Method for Acid Number of Petroleum Products by Potentiometric Titration*; ASTM International: West Conshohocken, PA, 2005.
(13) Tian, M.; Peng, X.; Feng, F.; Meng, S.; Fan, J.; Sun, S. *Dyes Pigments.* **2009**, *81*, 58.
(14) Wang, R.; Yu, C.; Yu, F.; Chen, L. *Trends Anal. Chem.* **2010**, *29*, 1004.
(15) Hamilton, G. R. C.; Sahoo, S. K.; Kamila, S.; Singh, N.; Kaur, N.; Hyland, B. W.; Callan, J. F. *Chem. Soc. Rev.* **2015**, *44*, 4415.
(16) Han, J.; Loudet, A.; Barhoumi, R.; Burghardt, R. C.; Burgess, K. *J. Am. Chem. Soc.* **2009**, *131*, 1642.
(17) Chen, Y.; Zhu, C.; Cen, J.; Bai, Y.; He, W.; Guo, Z. *Chem. Sci.* **2015**, *6*, 3187.
(18) Despras, G.; Zamaleeva, A. I.; Dardevet, L.; Tisseyre, C. *Chem. Sci.* **2015**, *6*, 5928.
(19) Chen, S.; Hong, Y.; Liu, Y.; Liu, J.; Leung, C. W. T.; Li, M.; Kwok, R. T. K.; Zhao, E.; Lam, J. W. Y.; Yu, Y.; Tang, B. Z. *J. Am. Chem. Soc.* **2013**, *135*, 4926.
(20) Kim, H. J.; Heo, C. H.; Kim, H. M. *J. Am. Chem. Soc.* **2013**, *135*, 17969.
(21) Han, J.; Burgess, K. *Chem. Rev.* **2010**, *110*, 2709.
(22) Bissell, R. A.; de Silva, A. P.; Gunaratne, H. Q. N.; Lynch, P. L. M.; Maguire, G. E. M.; Sandanayake, K. R. A. S. *Chem. Soc. Rev.* **1992**, *21*, 187.
(23) Fonrodona, G.; Ràfols, C.; Bosch, E.; Rosés, M. *Anal. Chim. Acta* **1996**, *335*, 291.
(24) This assumes that carboxylic acids are the only acidic species formed in the autoxidation, which will generally be true in the early stages of the reaction.
(25) Igarashi, J.; Jensen, R. K.; Lusztyk, J.; Korcek, S.; Ingold, K. U. *J. Am. Chem. Soc.* **1992**, *114*, 7727.
(26) We carried out ESI-MS in order to quantify acids produced during *n*-hexadecane autoxidations since it was a facile approach compared to acid-base titrations. This was enabled by the commercial availability of the linear carboxylic acid standards. Deuterated standards are preferred, but were unavailable. Accurate determination of acids beyond *ca.* 10 mM requires further sample dilutions due to ion saturation (accounting for the deviation between the two data points at

2500 seconds in Figure 2B).
(27) Furey, A.; Moriarty, M.; Bane, V.; Kinsella, B.; Lehane, M. *Talanta.* **2013**, *115*, 104.
(28) API Group III base oil is highly refined, severely hydrocracked crude oil that contains greater than 90% saturated hydrocarbon and a viscosity index >120.
(29) Chenier, J. H. B.; Tong, S. B.; Howard, J. A. *Can. J. Chem.* **1978**, *56*, 3047.
(30) Howard, J. A.; Ingold, K. U. *Can. J. Chem.* **1967**, *45*, 793.
(31) Jensen, R. K.; Korcek, S.; Zinbo, M. *Int. J. Chem. Kinet.* **1994**, 673.
(32) Zaikov, G. E.; Howard, J. A. *Can. J. Chem.* **1969**, *47*, 3017.
(33) Hanthorn, J. J.; Valgimigli, L.; Pratt, D. A. *J. Am. Chem. Soc.* **2012**, *134*, 8306.
(34) Hanthorn, J. J.; Valgimigli, L.; Pratt, D. A. *J. Org. Chem.* **2012**, *77*, 6908.
(35) Hanthorn, J. J.; Amorati, R.; Valgimigli, L.; Pratt, D. A. *J. Org. Chem.* **2012**, *77*, 6895.
(36) Valgimigli, L.; Pratt, D. A. *Acc. Chem. Res.* **2015**, *48*, 966.
(37) A similar BODIPY-based pH probe (see ref. 13) has been shown to undergo a 14-fold fluorescence enhancement upon protonation by acids in 1:1 EtOH:H_2O.
(38) Jensen, R. K.; Korcek, S.; Zinbo, M.; Gerlock, J. L. *J. Org. Chem.* **1995**, *60*, 5396.
(39) Friedmann Angeli, J. P.; Schneider, M.; Proneth, B.; Tyurina, Y. Y.; Tyurin, V. A.; Hammond, V. J.; Herbach, N.; Aichler, M.; Walch, A.; Eggenhofer, E.; Basavarajappa, D.; Rådmark, O.; Kobayashi, S.; Seibt, T.; Beck, H.; Neff, F.; Esposito, I.; Wanke, R.; Förster, H.; Yefremova, O.; Heinrichmeyer, M.; Bornkamm, G. W.; Geissler, E. K.; Thomas, S. B.; Stockwell, B. R.; O'Donnell, V. B.; Kagan, V. E.; Schick, J. A.; Conrad, M. *Nat. Cell Biol.* **2014**, *16*, 1180.
(40) Skouta, R.; Dixon, S. J.; Wang, J.; Dunn, D. E.; Orman, M.; Shimada, K.; Rosenberg, P. A.; Lo, D. C.; Weinberg, J. M.; Linkermann, A.; Stockwell, B. R. *J. Am. Chem. Soc.* **2004**, *136*, 4551.
(41) Autoxidations were carried out in the presence of 2,4,6-tri-tert-butylpyridine (1 mM) in order to prevent deactivation of 4 by acid formed during the autoxidation (see ref. 9).
(42) Pratt, D. A.; DiLabio, G. A.; Brigati, G.; Pedulli, G. F.; Valgimigli, L. *J. Am. Chem. Soc.* **2001**, *123*, 4625.
(43) Valgimigli, L.; Brigati, G.; Pedulli, G. F.; DiLabio, G. A.; Mastragostino, M.; Arbizzani, C.; Pratt, D. A. *Chem. Eur. J.* **2003**, *9*, 4997.
(44) Britto, N.; Gore, V. G.; Mali, R. S. *Synth. Commun.* **1989**, *19*, 1899.
(45) Lin, W.; Yuan, L.; Cao, Z.; Feng, J.; Feng, Y. *Dyes Pigments.* **2009**, *83*, 14.